Reactivity of Lattice Oxygens Present in V_2O_5(010): A Periodic First-Principles Investigation

Xilin Yin, Huanmei Han, Akira Endou, Momoji Kubo, Kazuo Teraishi, Abhijit Chatterjee, and Akira Miyamoto*

Department of Materials Chemistry, Graduate School of Engineering, Tohoku University, Aoba-yama 07, Aoba-ku, Sendai 980-8579, Japan

Received: June 16, 1998; In Final Form: November 13, 1998

The present paper deals with the periodic first-principles density functional (DFT) calculations on hydrogen adsorption on the V_2O_5(010) surface. The calculated results reveal that the vanadyl oxygen is the most active site for hydrogen adsorption among the three kinds of structurally different lattice oxygens in terms of their coordination with vanadiums. Our calculated harmonic vibrational frequencies of the three types of OH species are found to correlate with their corresponding bond strengths and support their respective reactivity. It is confirmed that the lattice relaxation contributes to the reactivity of the oxygens significantly in all cases while the local environment of adsorption site affects both the geometry and reactivity of the adsorption system only in the case of tricoordinated oxygen. Hydrogen adsorption at these oxygens reduces the surface in different ways. Comparison of the desorption ability of the OH species from the surface shows that removal of the O_1H species, formed by H adsorption at vanadyl oxygen, is energetically preferable. The present work demonstrates that the periodic approach gets rid of the artifacts of the cluster method, and thus, first-principles DFT methodology demonstrates its reliability to investigate geometric, electronic, and catalytic properties of transition metal oxide catalysts.

1. Introduction

Vanadium pentoxide (V_2O_5) is a very important material that has been extensively used as n-type semiconductors, cathode material in lithium batteries, and industrial catalysts.[1−3] It is mainly used as a catalyst in selective oxidation processes of hydrocarbons and sulfur dioxide, selective catalytic reduction (SCR) of nitric oxide by ammonia, and also photocatalytic reactions.[2−4] It is believed that the catalytic properties of a V_2O_5-based catalyst depend strongly on their ability to provide lattice oxygens for the reactions. Therefore, the investigation of the V_2O_5 lattice oxygen is crucial for understanding the active sites and reaction mechanisms. Three kinds of structurally different lattice oxygens exist in layered V_2O_5: singly coordinated O_1, which is a vanadyl oxygen (V═O species); dicoordinated O_2 and tricoordinated O_3, which bridge two and three vanadium atoms, respectively.[5]

One of the key steps in both selective oxidation of hydrocarbons[2] and SCR reactions[3] is the abstraction of an H atom from a reactant by one of the surface oxygens to form surface OH species. Hence, a study of adsorption of the H atom at V_2O_5 lattice oxygens is necessary to understand the active sites and reaction mechanisms. Furthermore, it is well-known that the interaction between reactant adsorbates and the surface is determined not only by the local chemical environment but also by the contribution of lattice relaxation. In this study, to rationalize the active oxygen sites as well as to study the influence of local environment and lattice relaxation, we performed the periodic first-principles density functional (DFT) calculations with respect to hydrogen adsorption.

Despite the extensive interest in V_2O_5 as a catalyst, some essential points regarding its active site in catalytic reactions still remain unresolved. Identification of the exact active site is one of the key issues, and different authors have proposed different active sites.[6−23] It has been generally accepted[6−16] that the vanadyl oxygen plays the most important role in catalysis. Tarama et al. has predicted for the first time the key role of the O_1 atom by studying the adsorption state on the V_2O_5 surface using infrared (IR) spectroscopy,[6] and later it has been widely supported by other experimental[7−12] and theoretical[13−16] workers. One of the present authors has investigated the selective oxidation of hydrocarbons and SCR of NO catalyzed by supported and unsupported V_2O_5 catalysts experimentally[10,11] and theoretically[15] and pointed out that the O_1 oxygen acts as the active site. Using an empirical formula, Andersson[13] calculated the electronic structure of V_2O_5 and suggested that the V═O species on the surfaces are responsible for the catalytic oxidation of hydrocarbons. Recently, employing the monolayer cluster model, Zhanpeisov et al.[14] have investigated the adsorption of both the H atom and proton on the V_2O_5 surface as well as the formation of oxygen vacancies by means of the SINDO1 approach. They concluded that the active site of V_2O_5 is probably associated with the O_1 site (terminal V═O group). Gilardoni et al.[16] have also proposed that the O_1 oxygen plays a key role in the SCR reactions from their calculations using a cluster model composed of two vanadiums.

In contrast to the aforementioned work regarding the most important role of the O_1 atom in catalysis, some authors have reported both from experiments[17,18] and theoretical calculations[19−22] that the O_2 oxygen participates in the catalytic process. Atomic force microscopy observation[17] revealed that the outermost (010) surface adsorbed by water molecules is not composed only of vanadyl oxygens. On the basis of this observation and previous theoretical studies as well as from simple geometrical considerations, they have inferred that the

* Corresponding author. Telephone: +81-22-217-7233. Fax: +81-22-217-7235. E-mail: miyamoto@aki.che.tohoku.ac.jp.

10.1021/jp982641a CCC: $18.00
Published on Web 02/06/1999

O_2 oxygen could act as the active site. Gasior et al.[18] have proposed that the O_2 oxygen plays the crucial role in SCR reactions. On the theoretical side, Witko and co-workers[19−22] have performed the semiempirical and ab initio calculations using the cluster approach. Their model clusters exhibit some artifacts: (1) the V−O bond lengths for all O atoms except for the O_1 atom were set equal to 1.83 Å, which is the respective average value in bulk V_2O_5; (2) the substrate unit of V_2O_5 was kept fixed at the geometry assumed by (1), ignoring the lattice relaxation; and (3) hydrogen was added in a direction perpendicular to the surface at each oxygen site, neglecting the influence of the local environment of the OH group. Owing to the above-mentioned reasons, their conclusion indicating the O_2 atom to be the active site becomes doubtful. So far, very few studies asserting that the O_3 atom acts as an active site have been reported. Using the semiempirical calculations, Ramirez et al.[23] have indicated that the most stable vacancy corresponds to the O_3 site rather than to the O_1 and/or O_2 site. Subsequently, they have found using IR data that the O_3 atoms participate more readily in the oxidation of dimethyl sulfoxide.

Mainly because of the limitations of experiments and also because of the restriction of computational techniques, the role of lattice oxygens present in V_2O_5 surface has not yet been clarified to formulate an understanding of the reactivity. Theoretically so far, studies concerning this issue have been performed by the cluster approach.[13−16] However, a difficult problem within the cluster approach for surface systems is the selection of size and shape of the model. Clusters provide a testing ground for the evaluation of surface properties, especially in small clusters where almost all atoms considered are surface atoms, although their coordination can be very different from surfaces of the corresponding bulk materials. Therefore, one must be aware of the artifacts that are introduced into the system by the calculation of physical parameters as functions of cluster size and geometry. Since the convergence to the bulk limit for the cluster and the adsorption is predictable by extrapolation with increasing cluster size, it was believed that such a large cluster can give reliable predictions.[24−26] However, in many cases, especially when cluster size is not large enough, the cluster approach may provide only a part of the reliable information, and it fails to supply comprehensive one. To have comprehensive predictions, one must attempt an artifact-free approach. Here, in heterogeneous catalysis, the periodic boundary method was found to be able to rid the problem associated with the localized cluster approach for surface systems.[27−33] Such an attempt of course would require far more computational effort than is needed for the application of the cluster approach.

In recent years, with the rapid development of computational techniques, it has become feasible to deal with the adsorption systems using periodic boundary first-principles calculations. Our previous study[29] shows that the periodic DFT approach is very reliable for investigating V_2O_5, since the results are in very good agreement with experimental observations.

The present work is organized as follows. In section 2 we describe the computational details and model, and section 3 presents the results and discussion, which include a comparison and evaluation of the systematic optimization techniques. Finally, section 4 summarizes the highlights of this paper.

2. Methodology

2.1. Computational Details. The periodic DFT calculations were performed using the DSolid program[34] within the Kohn−Sham formalism.[35] In this program one-electron Schrödinger equations are solved only at the $k = 0$ wave vector point of the Brillouin zone. This program can be applied to systems that have small unit cells simply by ignoring this and treating them as having a larger cell, as described in the DSolid User Guide.[34] We used the Vosko−Wilk−Nusair local type functional (LDA)[36] for the geometry optimizations, whereas the interaction energies were computed using the Becke−Lee−Yang−Parr nonlocal type functional (NLDA)[37,38] that contains the necessary gradient corrections to eliminate the inaccuracies of the LDA for the estimations of the energy differences. Molecular orbitals were expanded into a set of numerical atomic orbitals of doubly numerical + polarization (DNP) quality provided by the software package. The DNP is comparable in quality to Pople's split-valence 6-31G** basis set and usually yields the most reliable results.[39−41] To eliminate convergence problems in some cases, we allowed partial occupancies for the high-lying orbitals using smear values of less than 0.02 eV. For the numerical integration we used the MEDIUM quality mesh size of the program. To reduce the necessary CPU time, we froze the inner-core orbitals of the atoms except for hydrogen, whose pure potential was used; i.e., 1s was frozen for oxygen and 1s2s2p for vanadium. For geometry optimization, the BFGS routine in which the gradients were computed numerically was employed. The tolerances of energy and gradient convergence are used as their default values: 1.0×10^{-6} and 2.0×10^{-3}. We have also performed the vibrational frequency calculations at the LDA level using the LDA-optimized structures. Two-point differencing and a step size of 0.01 were used.

2.2. Model. Owing to the importance in catalysis mainly, the real structure of V_2O_5(010) has been discussed well in the literature.[12,13,20−22,42−50] Experimental studies show that V_2O_5-(010) plays a key role in catalysis[51,52] and that the supported (010) monolayer has excellent catalytic activity.[53,54] Experimental[47] and theoretical[29,31] studies demonstrate that the (010) surface has very similar physical properties and stability compared with its bulk crystal. Therefore, we considered V_2O_5-(010) for our present study. The surface has been modeled by a periodic slab composed of single unit cell (SUC) monolayer that has been successfully employed for band calculations,[29−33] as shown in Figure 1, where the optimized lattice parameters of *a* (11.535 Å) and *c* (3.603 Å) obtained by the CASTEP program were used.[29] The successive slabs along the *b* axis are separated by a vacuum region. The shortest distance between atoms belonging to successive slabs is greater than 8.3 Å, where the interlayer interaction is not significant.

The large unit cell (LUC) method,[55−60] which is mainly investigated by Evarestov and co-workers,[55−58] is believed to be better than the SUC one. Accordingly, it needs much more computational effort for the LUC calculations. Since a V_2O_5 unit cell consists of 14 atoms, even the smallest LUC model contains 28 atoms, including 8 vanadiums and 20 oxygens and excluding adsorbate atom(s). Such calculations consume enormous time. To understand the difference between the LUC and SUC methods, we made the LUC model, which is twice the V_2O_5(010) unit cell monolayer, by doubling the lattice parameter *c* (3.603 Å) and performed the calculations. As predicted, the obtained bond lengths and atomic charges (Tables 1 and 2) show that some differences exist between the two models with different sizes; however, the differences are not significant. In particular, the ordering of the bond lengths and atomic charges were found to be the same in the case of SUC. This indicates that the SUC model used in the present study is found to be a good compromise between cost and accuracy.

To investigate the influence of the V_2O_5(010) sublayer on the geometric and electronic structures quantitatively, we have

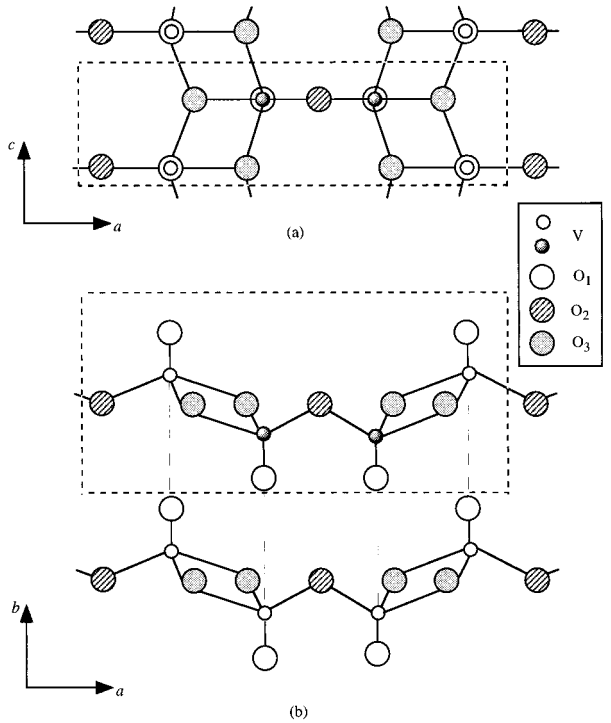

Figure 1. Periodic boundary model of V_2O_5(010) used in the present study is indicated by broken lines, projection onto (a) the *ac* plane and (b) the *ab* plane. The closed small circles represent the exposed V atoms on the surface, and the opened small ones designate the V atoms beneath the singly coordinated oxygens.

TABLE 1: O−V Bond Lengths (Å) in V_2O_5(010) Monolayer Composed of the Single Unit Cell (SUC) and Large Unit Cell (LUC)

bond	O_1−V	O_2−V	O_3−V	O_3−V
SUC (Å)	1.57	1.74	1.97	2.04
LUC (Å)	1.57	1.78	1.91	2.03

TABLE 2: Mulliken Atomic Charges (au) of V_2O_5(010) Monolayer Made Up of the SUC and LUC

atoms	O_1	O_2	O_3	V
SUC	−0.324	−0.602	−0.646	+1.272
LUC	−0.301	−0.610	−0.709	+1.315

also performed calculations using a bilayer slab composed of one unit cell. The following points were justified through the obtained results (Tables 3 and 4). (1) For the clean bilayer surface, no significant differences of both the V−O bond lengths and atomic charges are observed between the monolayer and bilayer slabs, and the ordering of the bilayer values is in good agreement with that of the monolayer slab. (2) Similarly for the adsorption systems, the major geometrical parameters and atomic charges are also very close to those of the monolayer. In particular, the ordering of the bilayer results almost remains the same as that of the monolayer model. All these good agreements show that our monolayer slab is sufficient for studying the interaction with hydrogen, although little difference was found when the thickness of the slab was increased.

Therefore, the SUC monolayer slab used in the current study can be considered approximately as a realistic model of V_2O_5-(010) for the investigation of hydrogen adsorption.

3. Results and Discussion

To investigate the effect of both the local environment of an adsorption site and lattice relaxation, systematic optimization methods were adopted: (I) optimization of the *z*-coordinates of the H atom and its corresponding adsorption site, i.e. the O−H group, constraining these two atoms in an orientation perpendicular to the surface plane, and in this case, other atoms of the adsorbate−substrate system are fixed and the geometry remains identical to that of the clean (010) surface; (II) optimization of all three coordinates of the O−H group using former equilibrium geometries in order to examine the influence of the local chemical environment of the adsorption site; (III) full optimization of all the constituent atoms of the adsorbate−substrate system, based on the geometries obtained by optimization II, to examine the contribution of lattice relaxation.

TABLE 3: Selected Bond Lengths (Å) Obtained by Using Monolayer and Bilayer SUC of V_2O_5(010)[a]

adsorption sites	bonds	I	II	III	clean surface
O_1 site	O_1−H	0.97 (0.97)	0.97 (0.97)	0.97 (0.97)	
	O_1−V	1.68 (1.70)	1.69 (1.70)	1.70 (1.70)	1.57 (1.56)
O_2 site	O_2−H	0.98 (0.98)	0.98 (0.98)	0.98 (0.98)	
	O_2−V	1.85 (1.83)	1.85 (1.83)	1.90 (1.89)	1.74 (1.75)
	O_2−V	1.85 (1.83)	1.85 (1.83)	1.90 (1.89)	1.74 (1.75)
O_3 site	O_3−H	0.99 (0.99)	0.99 (0.99)	0.99 (0.99)	
	O_3−V	1.99 (2.02)	2.16 (2.31)	2.25 (2.30)	2.04 (2.04)
	O_3−V	2.01 (2.00)	1.99 (1.99)	2.00 (2.00)	1.97 (1.97)
	O_3−V	2.01 (2.00)	1.99 (1.99)	2.00 (2.00)	1.97 (1.97)
	H−O_2[b]	3.00 (3.00)	2.32 (2.24)	2.29 (2.23)	

[a] Bilayer results are shown in parenthesesbrackets. Three types of optimization methods were employed: (I) *z* coordinates of OH group, (II) all three coordinates of OH group, and (III) full geometry including all atoms. [b] This atom is the closest neighbor of the O_3 site among dicoordinated oxygens.

The adsorption energy (E_{ads}) has been calculated according to the expression

$$E_{ads} = E_{(adsorbate-substrate)} - (E_{adsorbate} + E_{substrate})$$

where $E_{(adsorbate-substrate)}$, $E_{adsorbate}$, and $E_{substrate}$ are the total energies of the adsorbate−substrate system, isolated adsorbate, and isolated substrate, respectively. A negative E_{ads} value corresponds to a stable adsorbate−substrate system.

3.1. Reactivity of Lattice Oxygens. The results obtained from the three different optimization conditions show that all three lattice oxygens have high reactivity for H adsorption and that the O_1 site is found to be the most active (Table 5), which is in line with the experimental identification.[6−12]

Although there are rather significant differences in reactivity of these oxygen sites after optimization I, these differences cannot reflect the realistic situation precisely, since the contribution of neither local environment nor lattice relaxation was taken into account. After the optimization II, the reactivity of O_1 and O_3 atoms is found to be very close. In particular, no significant difference is found in the reactivity of the three types of oxygens after full geometry optimization III (see Table 5). It was confirmed that the O_1 site acts as the active site in an unsupported V_2O_5 catalyst. Regarding the supported catalyst, however, the situation is different more or less. Since the support and/or promoter of catalyst may change the geometric and electronic structures of V_2O_5, which greatly affect the adsorption state, and considering that no significant adsorption energy difference at the three O sites of unsupported V_2O_5 is found, one can say that the reactivity ordering of these oxygens may be changed for supported V_2O_5 catalyst in some cases.

Now the results obtained from all the three optimization conditions are compared. Between optimizations I and II, there is no significant difference for H adsorption at the O_1 site, as

TABLE 4: Selected Mulliken Atomic Charges (au) Calculated by Using Monolayer and Bilayer SUC of V_2O_5(010)[a]

adsorption sites	atoms	I	II	III	clean surface
O_1 site	H	+0.303 (+0.296)	+0.303 (+0.291)	+0.300 (+0.296)	
	O_1	−0.490 (−0.491)	−0.490 (−0.487)	−0.511 (−0.510)	−0.324 (−0.305)
	V	+1.279 (+1.266)	+1.272 (+1.268)	+1.275 (+1.240)	+1.272 (+1.236)
O_2 site	H	+0.394 (+0.394)	+0.391 (+0.392)	+0.388 (+0.386)	
	O_2	−0.607 (−0.652)	−0.604 (−0.652)	−0.567 (−0.577)	−0.602 (−0.596)
	V	+1.195 (+1.259)	+1.195 (+1.258)	+1.180 (+1.252)	+1.272 (+1.335)
	V	+1.195 (+1.259)	+1.195 (+1.258)	+1.180 (+1.252)	+1.272 (+1.335)
O_3 site	H	+0.440 (+0.439)	+0.431 (+0.414)	+0.421 (+0.413)	
	O_3	−0.670 (−0.652)	−0.643 (−0.604)	−0.621 (−0.590)	−0.646 (−0.619)
	V	+1.137 (+1.159)	+1.200 (+1.228)	+1.280 (+1.251)	+1.272 (+1.236)
	V	+1.180 (+1.289)	+1.128 (+1.208)	+1.153 (+1.237)	+1.272 (+1.335)
	V	+1.180 (+1.289)	+1.128 (+1.208)	+1.153 (+1.237)	+1.272 (+1.335)
	O_2[b]	−0.576 (−0.630)	−0.635 (−0.691)	−0.673 (−0.671)	−0.602 (−0.596)

[a] Bilayer values are listed in parenthesesbrackets. The optimization conditions used were described in Table 3. [b] See Table 3.

TABLE 5: Adsorption Energies of H Atom at O_1, O_2, and O_3 Oxygen Sites Present in Monolayer SUC of V_2O_5(010) Calculated by the Aforementioned Optimization Methods

optimization methods	I	II	III
E_{ads}, O_1 (kcal/mol)	−47.1	−46.4	−62.2
E_{ads}, O_2 (kcal/mol)	−39.9	−39.0	−60.3
E_{ads}, O_3 (kcal/mol)	−32.0	−45.8	−59.3

well as at the O_2 site. This indicates that there is almost no effect of local environment at both O_1 and O_2 sites on their reactivity. However, the O_3 site exhibits completely different behavior. For optimization condition II, H atom binding to the O_3 site also interacts with its nearest O_2 site with a hydrogen bond. As a consequence, the adsorption energy is negatively increased by 13.8 kcal/mol. It shows that the local chemical environment of the O_3 site affects both geometry and energy.

On the other hand, a remarkable difference is observed after full geometry optimization at both O_1 and O_2 sites. A negative increment of adsorption energy of 15.8 and 21.3 kcal/mol was calculated, respectively. These comparatively higher energy differences show the significant contribution of lattice relaxation on adsorption systems with respect to both the O_1 and O_2 sites. Similarly, full geometry optimization for H adsorption at the O_3 site also leads to a negative increment of adsorption energy by 13.5 kcal/mol where the surface relaxation is the main contributor.

3.2. Geometric Structures. Equilibrium geometries of the adsorption systems obtained by the respective optimization methods are shown in Figures 2−4. The selected bond lengths between adsorption sites and their closest neighbors are shown in Table 3. It is observed that the surface relaxation has significant effect. At all the three optimizations, equilibrium bond lengths of the O−H group increase in the order O_1−H < O_2−H < O_3−H, indicating that the bonding of O_1−H is the strongest, which further corresponds to the highest reactivity of the vanadyl oxygen. On the other hand, no significant change in the O_1−H bond length is observed after all the three types of optimizations. The same is true for both O_2−H and O_3−H bonds. This justifies again that lattice relaxation contributes significantly to the adsorption energy and not to the newly forming O−H bonds.

As described above, geometry optimization with step II for the O_3 site shows that a hydrogen bond is formed between the H and its closest neighbor O_2 atom with a distance of 2.32 Å (Figure 3c). This H-bond almost remains unaltered after the full geometry optimization (step III), which indicates that the lattice relaxation has no pronounced influence on the H-bond (Figure 4c) either. To form this hydrogen bond, one V−O_3 bond has been elongated significantly while the other two identical V−O_3 bonds almost have not shown any significant changes (Table 3). In contrast, the local environment of either the O_1 or the O_2 site hardly affects the geometry.

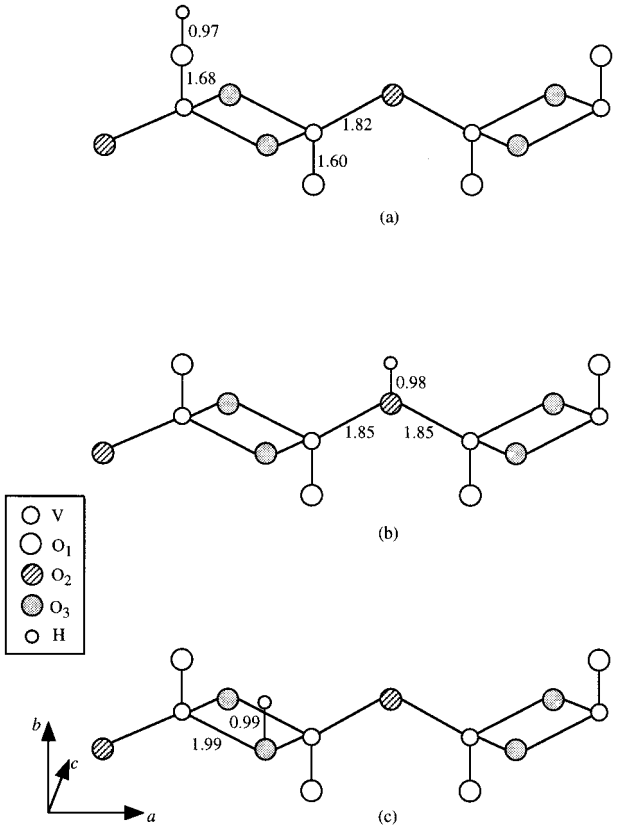

Figure 2. Geometries of hydrogen adsorption at (a) O_1, (b) O_2, and (c) O_3 oxygen sites on V_2O_5(010) obtained by optimizing the z coordinates of OH species. The values shown here denote the bond lengths (Å).

3.3. Electronic Structures. Major atomic charges of the respective adsorption systems are shown in Table 4. For all the optimization conditions, the charge on the H atom increases with the order of the corresponding adsorption site: O_1 < O_2 < O_3, which shows the trend of their depleting electron from H atom.

In the step I optimization, adsorption sites accumulate the electrons; the most significant accumulation is found at the O_1 site. The V atoms bonded to the O_2 and O_3 sites are observed to be reduced, whereas the V atom bound to the O_1 site has a charge almost identical to that of the clean surface, and the other vanadiums are reduced rather significantly instead.

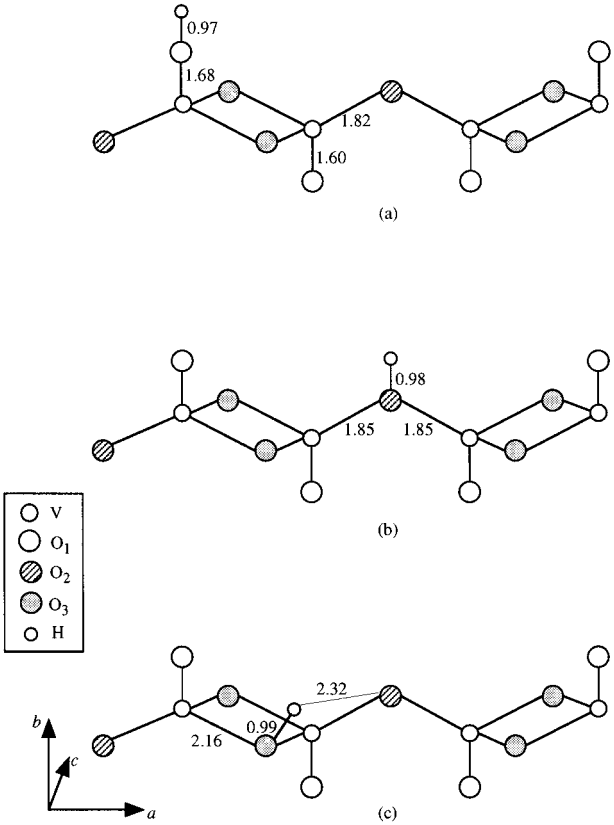

Figure 3. Geometries of hydrogen adsorption at (a) O_1, (b) O_2, and (c) O_3 oxygen sites on V_2O_5(010) obtained by optimizing all three coordinates of OH species. The values shown here denote the bond lengths (Å).

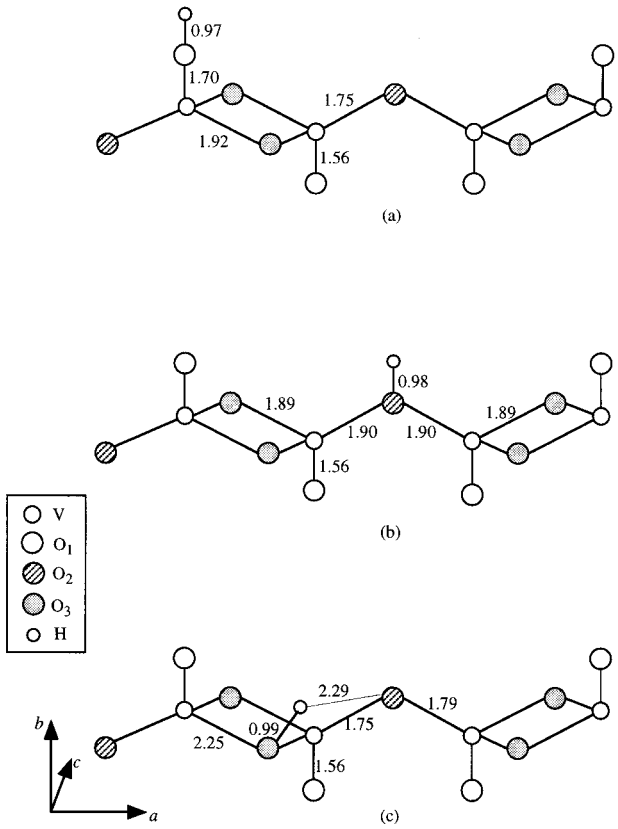

Figure 4. Fully optimized geometries of hydrogen adsorption at (a) O_1, (b) O_2, and (c) O_3 oxygen sites on V_2O_5(010). The values shown here denote the bond lengths (Å).

Electronic structures obtained by optimization II are compared with that of optimization I. Atomic charges on both the O_1 and O_2 sites remain almost the same under both conditions. In the case of O_3, however, a significant change is observed. At this site, charges on the H and O_3 atoms are decreased, charges on one V atom is increased by 0.063 e, while those on the other two V atoms that are located in the same local environment are decreased by 0.052 e. Since the H-bond was formed between the H bound to O_3 site and its closest O_2 atom, the charge on this O_2 increased correspondingly.

At the full optimization (step III), charge redistribution occurs when compared to that of the former two optimization methods. Charges on both the O_2 and O_3 sites are depleted remarkably; however, the O_1 site has accumulated more charge. Our previous investigation of the V_2O_5(010) surface[29] has revealed that the vanadyl oxygen is the least ionic among these three oxygens, which shows that the O_1 site still has potential to gain extra electrons, and hence, the O_1 site exhibits a different behavior. Simultaneously, the charge on the V atom beneath the adsorption site O_1 is almost identical to that of the clean surface, while the other three V atoms get reduced instead. On the other hand, the two V atoms bonded to the O_2 site and the two V atoms closer to the O_3 site are observed to get reduced very significantly in the cases of adsorption at O_2 and O_3 sites, respectively.

3.4. Vibrational Frequencies of the Surface Hydroxyl Species. The spectra of hydroxyl groups raise a question regarding the location of the groups. What is the nature of the local surface environment responsible for their differences in frequency and in chemical behavior?[61] As catalytically important Brönsted acid sites, hydroxyl groups play a key role in the catalysis process. Bond et al.[62] revealed that the vibrational frequency of surface OH groups on V_2O_5 ranges from 3300 to 3700 cm^{-1} by means of IR study. Although some authors[9,63] pointed out that the surface hydroxyl species connected to the O_1 atom shows a frequency of 3648 or 3645 cm^{-1}, there are very few reports with respect to the frequencies of O_2H and O_3H species in the literature. To elucidate their difference, harmonic vibrational frequencies are evaluated on the fully optimized geometries. Since the anharmonic vibrational frequency is not included, overestimation of the frequency is reasonable.

Our calculated vibrational frequencies of the O_1H, O_2H, and O_3H groups are 3792.17, 3658.26, and 3561.13 cm^{-1}, respectively, which indicates that the least coordinated hydroxyl of O_1H shows the highest frequency value and that the most coordinated hydroxyl of O_3H exhibits the lowest one. This trend is very consistent with that of the hydroxyl species present in the alumina surface.[64] Also, these values are almost within the range of the observation of Bond and co-workers.[62] In particular, the calculated frequency of the O_1H group is very close to the experimental values,[9,63] which again justified our methodology. Furthermore, it is found that these frequencies correlate with the reactivity of the surface oxygens as well as with the bond strengths of the hydroxyl species.

3.5. Desorption Ability of the Surface Hydroxyl Species. The reactivity of surface oxygens depends not only on their adsorption ability but also on their desorption ability of the hydroxyl group from the surface to form the OH^- species and O vacancy. A series of calculations were performed to evaluate the desorption ability. The obtained potential curves describing the desorption of surface OH species obtained by optimization condition I are shown in Figure 5. The OH desorption process was investigated by keeping the surface and OH group fixed at

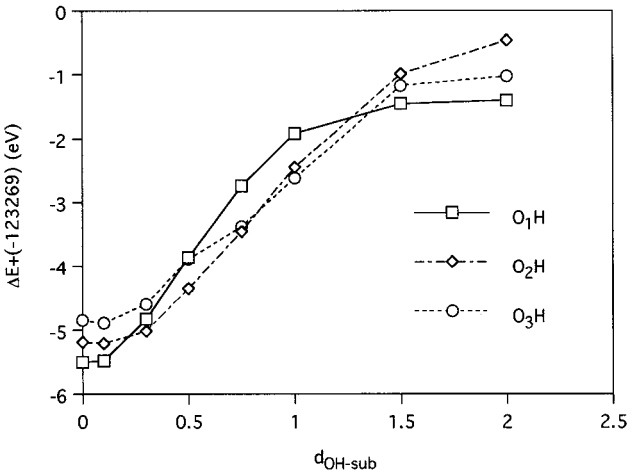

Figure 5. Potential curves describing the desorption of surface OH species obtained by optimizing the *z* coordinates of OH group. d_{OH-sub} represents the distance between the hydroxyl O atom and its equilibrium position of 0.0 Å. The value of [$\Delta E+$ (−123 269) (eV)] corresponds to the total energy of adsorption systems.

their equilibrium coordinates, respectively, and varying only the position of the OH species particularly on the surface. The potential was described by the distance d_{OH-sub} between the hydroxyl O atom and its equilibrium position. The results (Figure 5) show that the O_1H and O_3H species essentially reach their free positions where they are out of the interaction with the (010) surface when the distance reached is 2.0 Å, whereas the O_2H species still has significant interaction with the surface. From their equilibrium of 0.0 Å to the position of 2.0 Å, energy differences are found to be 4.100, 4.727, and 3.819 eV corresponding to O_1H, O_2H, and O_3H, respectively. These correspond to the minimum energies that should be exerted to remove the respective OH species from the equilibrium adsorption system. These values demonstrate that removal of the O_3H species is the most favorable energetically in the case of optimization condition I, but practically, it is necessary to overcome the energy of ca. 0.6 eV contributed by the H-bonding, as discussed above. Thus, removal of the O_1H species from the (010) surface is found to be the cheapest energetically if one considers the effect contributed by the local environment of adsorption site.

It was found that H adsorption, OH desorption, and O vacancy formation are correlated processes. This investigation indicates that the vanadyl oxygen not only has the strongest binding ability on H atom but also the greatest desorption ability of hydroxyl group to form the OH^- species and oxygen vacancy.

4. Conclusions

We performed the first-principles DFT calculations under the periodic boundary condition to rationalize the active oxygen sites of V_2O_5, as well as to study the influence of local environment and lattice relaxation on reactivity. The major conclusions obtained from the calculations are as follows. Vanadyl oxygen (singly coordinated O_1) acts as the most active site toward hydrogen adsorption among the three kinds of lattice oxygens present in unsupported V_2O_5(010), in good agreement with many experimental observations. Lattice relaxation contributes to the reactivity of the surface oxygens significantly in all cases, while the local environment of the adsorption site affects both geometry and reactivity of the adsorption system only for tricoordinated oxygen. Hydrogen adsorption reduces the surface, whereas the adsorption at O_1 shows different behavior; the O_1 site accumulates much charge, and the V atom beneath the O_1 is almost identical to that of clean surface, while the other three V atoms get reduced. The calculated harmonic vibrational frequencies reveal the difference among the three types of hydroxyl species and correlate with bond strengths as well as support their reactivity. When the influence of the local environment of the adsorption site is considered, desorption of the O_1H species from V_2O_5(010) is the cheapest energetically. It is found that the processes of H adsorption, OH desorption, and O vacancy formation are correlated. The present study indicates that the periodic approach rids the artifacts of the cluster method and that the periodic first-principles DFT methodology is found to be reliable for investigating not only geometric and electronic structures but also the reactivity of transition metal oxide catalysts.

References and Notes

(1) Whittingham, M. S. *J. Electrochem. Soc.: Electrochem. Sci. Technol.* **1976**, *123*, 315.
(2) Grzybowska-Swierkosz, B. *Appl. Catal. A* **1997**, *157*, 263.
(3) Bosch, H.; Janssen, F. *Catal. Today* **1988**, *2*, 369.
(4) Mars, P.; Maessen, J. G. H. *J. Catal.* **1968**, *10*, 1.
(5) In this paper, we index V_2O_5 using the conventional setting. We note that there is a frequent inversion of the *b* and *c* axes in different studies.
(6) Tarama, K.; Yoshida, S.; Ishida, S.; Kakioka, H. *Bull. Chem. Soc. Jpn.* **1968**, *41*, 2840.
(7) Andersson, A. *Adsorption and Catalysis on Oxide Surface*; Che, M., Bond, G. C., Eds.; Elsevier: Amsterdam, 1985.
(8) Ozkan, U. S.; Cai, Y.; Kumthekar, M. W. *J. Catal.* **1994**, *149*, 375.
(9) Topsøe, N.-Y.; Dumesic, J. A.; Topsøe, H. *J. Catal.* **1995**, *151*, 241.
(10) Inomata, M.; Miyamoto, A.; Murakami, Y. *J. Catal.* **1980**, *62*, 140.
(11) Mori, K.; Miyamoto, A.; Murakami, Y. *J. Phys. Chem.* **1985**, *89*, 4265.
(12) Zhang, Z.; Henrich, V. E. *Surf. Sci.* **1994**, *321*, 133.
(13) Andersson, A. *J. Solid State Chem.* **1982**, *42*, 263.
(14) Zhanpeisov, N. U.; Bredow, T.; Jug, K. *Catal. Lett.* **1996**, *39*, 111.
(15) Miyamoto, A.; Inomata, M.; Hattori, A.; Ui, T.; Murakami, Y. *J. Mol. Catal.* **1982**, *16*, 315.
(16) Gilardoni, F.; Weber, J.; Baiker, A. *Intl. J. Quantum Chem.* **1997**, *61*, 683.
(17) Da Costa, A.; Mathieu, C.; Barbaux, Y.; Poelman, H.; Dalmai-Vennik, G.; Fiermans, L. *Surf. Sci.* **1997**, *370*, 339.
(18) Gasior, M.; Haber, J.; Machej, T.; Czeppe, T. *J. Mol. Catal.* **1988**, *43*, 359.
(19) Witko, M.; Tokarz, R.; Haber, J. *J. Mol. Catal.* **1991**, *66*, 205.
(20) Witko, M.; Hermann, K.; Tokarz, R. *J. Electron. Spectrosc. Relat. Phenom.* **1994**, *69*, 89.
(21) Witko, M.; Tokarz, R.; Haber, J. *Appl. Catal. A* **1997**, *157*, 23.
(22) Michalak, A.; Witko, M.; Hermann, K. *Surf. Sci.* **1997**, *375*, 385.
(23) Ramirez, R.; Casal, B.; Utrera, L.; Ruiz-Hitzky, E. *J. Phys. Chem.* **1990**, *94*, 8960.
(24) Jug, K.; Geudtner, G. *Chem. Phys. Lett.* **1993**, *208*, 537.
(25) Bredow, T.; Jug, K. *Chem. Phys. Lett.* **1994**, *223*, 89.
(26) Jug, K.; Geudtner, G. *J. Mol. Catal. A* **1997**, *119*, 143.
(27) Koutecky, J.; Fantucci, P. *Chem. Rev.* **1986**, *86*, 539.
(28) Hermann, K.; Bagus, P. S.; Nelin, C. J. *Phys. Rev. B* **1987**, *35*, 9467.
(29) Yin, X.; Fahmi, A.; Endou, A.; Miura, R.; Gunji, I.; Yamauchi, R.; Kubo, M.; Chatterjee, A.; Miyamoto, A. *Appl. Surf. Sci.* **1998**, *130*−*132*, 539.
(30) Lambrecht, W.; Djafari-Rouhani, B.; Lannoo, M.; Vennik, J. *J. Phys. C* **1980**, *13*, 2485.
(31) Lambrecht, W.; Djafari-Rouhani, B.; Vennik, J. *J. Phys. C* **1981**, *14*, 4775.
(32) Georing, E.; Müller, O.; Klemm, M.; denBoer, M. L.; Horn, S. *Philos. Mag. B* **1997**, *75*, 229.
(33) Eyert, V.; Höck, K.-H. *Phys. Rev. B* **1998**, *57*, 12727.
(34) *DSolid User Guide*; Molecular Simulations: San Diego, September 1996.
(35) Kohn, W.; Sham, L. J. *Phys. Rev. A* **1965**, *140*, 1133.
(36) Vosko, S. H.; Wilk, L.; Nusair, M. *Can. J. Phys.* **1980**, *58*, 1200.
(37) Becke, A. D. *J. Chem. Phys.* **1988**, *88*, 2547.
(38) Lee, C.; Yang, W.; Parr, R. G. *Phys. Rev. B* **1988**, *37*, 786.
(39) Frisch, M. J.; Pople, J. A.; Binkley, J. S. *J. Chem. Phys.* **1984**, *80*, 3265.
(40) Gordon, M. S.; Binkley, J. S.; Pople, J. A.; Pietro, W. J.; Hehre, W. J. *J. Am. Chem. Soc.* **1982**, *104*, 2797.

(41) Francl, M. M.; Pietro, W. J.; Hehre, W. J.; Binkley, J. S.; Gordon, M. S.; Defrees, D. J.; Pople, J. A. *J. Chem. Phys.* **1982**, *77*, 3654.
(42) Witko, M.; Hermann, K.; Tokarz, R.; Michalak, A. 213th ACS National Meeting, San Francisco, 1997; Abstract PETR 074.
(43) Hermann, K.; Michalak, A.; Witko, M. *Catal. Today* **1996**, *32*, 321.
(44) Fiermans, L.; Clauws, P.; Lambrecht, W.; Vandenbroucke, L.; Vennik, J. *Phys. Status Solidi A* **1980**, *59*, 485.
(45) Lambrecht, W.; Djafari-Rouhani, B.; Vennik, J. *Solid State Commun.* **1981**, *39*, 257.
(46) Lambrecht, W.; Djafari-Rouhani, B.; Vennik, J. *J. Phys. C* **1986**, *19*, 369.
(47) Poelman, H.; Vennik, J.; Dalmai, G. *J. Electron. Spectrosc. Relat. Phenom.* **1987**, *44*, 251.
(48) Smith, R. L.; Lu, W.; Rohrer, G. S. *Surf. Sci.* **1995**, *322*, 293.
(49) Smith, R. L.; Rohrer, G. S.; Lee, K. S.; Seo, D.-K.; Whangbo, M.-H. *Surf. Sci.* **1996**, *367*, 87.
(50) Oshio, T.; Sakai, Y. *J. Vac. Sci. Technol. B* **1994**, *12*, 2055.
(51) Inomata, M.; Miyamoto, A.; Murakami, Y. *J. Phys. Chem.* **1981**, *85*, 2372.
(52) Inomata, M.; Mori, K.; Miyamoto, A.; Ui, T.; Murakami, Y. *J. Phys. Chem.* **1983**, *87*, 754.
(53) Saleh, R. Y.; Wachs, I. E.; Chan, S. S.; Chersich, C. C. *J. Catal.* **1986**, *98*, 102.
(54) Bond, G. C. *Appl. Catal. A* **1997**, *157*, 91.
(55) Dobrotvorskii, A. M.; Evarestov, R. A. *Vestn. Leningr.. Univ.* **1972**, *22*, 45.
(56) Evarestov, R. A.; Petrashen, M. I.; Ledovskaya, E. M. *Phys. Status Solidi B* **1975**, *68*, 453.
(57) Evarestov, R. A.; Smirnov, V. P. *Phys. Status Solidi B* **1983**, *119*, 9.
(58) Evarestov, R. A.; Smirnov, V. P. *Phys. Status Solidi B* **1997**, *201*, 75.
(59) Bennett, A. J.; McCarroll, B.; Messmer, R. P. *Phys. Rev. B* **1971**, *3*, 1397.
(60) Lindefelt, U. *J. Phys. C* **1978**, *11*, 85.
(61) Peri, J. B. *Infrared Spectroscopy in Catalytic Research*; Catalysis: Science and Technology 5; Anderson, J. R., Boudart, M., Eds.; Springer-Verlag: Berlin, 1984.
(62) Bond, G. C.; Sárkány, A. J.; Parfitt, G. D. *J. Catal.* **1979**, *57*, 476.
(63) Busca, G.; Ramis, G.; Lorenzolli, V. *J. Mol. Catal.* **1989**, *50*, 231.
(64) Morterra, C.; Magnacca, G. *Catal. Today* **1996**, *27*, 497.